

Sn(II)/PN@AC catalysts: synthesis, physical-chemical characterization, and applications

Yibo WU^{1,2} , Fuxiang LI^{2*} , Qinbin LI¹ , Yongjun HAN¹ , Li WANG¹ , Wei MA¹ , Fu XV¹ 

¹College of Chemistry and Environmental Engineering, Pingding Shan University, Pingding Shan, China

²College of Chemistry and Chemical Engineering, Taiyuan University of Technology, Taiyuan, China

Received: 08.03.2021 • Accepted/Published Online: 28.06.2021 • Final Version: 19.10.2021

Abstract: In this study, the novel tin-based catalysts (Sn(II)/PN@AC) were prepared using the phosphorus and nitrogen dual-modified activated carbon as support and SnCl₂ as active compounds, as well as then evaluated in acetylene hydrochlorination. Under the reaction temperature of 180 °C and an acetylene gas hourly space velocity (GHSV-C₂H₂) of 30 h⁻¹, the 15%Sn(II)/PN@AC-550 showed the initial acetylene conversion of 100% and vinyl chloride selectivity over 98.5%. Additionally, the deactivation rate of 15%Sn(II)/PN@AC-550 reached 0.47% h⁻¹, which was lower than that of 15%Sn(II)/AC-550 (1.02% h⁻¹), suggesting that PN@AC-550 as novel support can retard the deactivation of Sn(II)/AC-550 catalysts during acetylene hydrochlorination. Based on the catalytic tests and characterization results (XRD, Raman, BET surface area, TEM, C₂H₂-TPD, H₂-TPR, XPS, FT-IR, TGA, and ICP), it demonstrated that PN@AC-550 as support could effectively improve the dispersion of tin species, retard the formation of coke deposition, lessen the oxidation of SnCl₂ during the preparation process, as well as relatively inhibit the leach of tin species during the reaction. By combing the FTIR results and Rideal–Eley mechanism, we proposed that that HSnCl₃ was transition state of SnCl₂ in catalysis acetylene hydrochlorination and then adsorbed the acetylene to produce the vinyl chloride.

Key words: Tin-based catalysts; nitrogen elements; phosphorus elements; acetylene hydrochlorination

1. Introduction

Tin-based catalysts for diverse application includes electrochemical CO₂ reduction [1] and acetylene hydrochlorination (reaction equation: H₂C=CH₂+HCl=H₂C=CHCl) [2–4], the latter of which is a significant technology to manufacture vinyl chloride. Despite the initial activity of tin-based catalysts is close to traditional mercury-based acetylene hydrochlorination catalysts, there is still an ongoing study in prolonging the lifetime. The tin-based acetylene hydrochlorination catalysts can be classified into three categories: bimetallic or multimetallic tin-based catalysts [2–8], organotin-based catalysts [9–11], and tin complex-based catalysts [4,12]. Given the easily sublimation of SnCl₄ under industrially relevant process conditions [2], the efficient durability of SnCl₄/AC in acetylene hydrochlorination can be prolonged by the incorporation of BiCl₃ and CoCl₂ [8]. Moreover, the Kocheshkov redistribution reaction of SnCl₄ and Ph₃ClSn can further improve the catalytic behavior of SnCl₄/AC [10]. Later on, Guo et al. founded that the synergistic effect of SnCl₂, ZnCl₂, and Tb₄O₇ can strengthen stability of SnCl₂/AC in acetylene hydrochlorination [5]. In the previous work, we founded that SnCl₂/AC is easily oxidized during preparation process, but Li-Sn(IV) in LiSnCl_n/AC is structurally stable, enhancing the stability of SnCl₂/AC in acetylene hydrochlorination [3]. Moreover, based on the Rideal–Eley mechanism and the previous study and mentioned above results, we can infer that HSnCl₃ is a transition state of tin active sites and then adsorbed the acetylene to produce the vinyl chloride [3]. Additionally, the lifetime of SnCl₂/AC catalysts in acetylene hydrochlorination can be also elevated via the coordination interaction of organic linkage and Sn sites [4,11].

Owing to the dispersion of Cu species on catalysts surface keeps the direct relation with P doping, Cu-P/AC catalysts displays longer lifetime as compare to CuCl₂/AC in acetylene hydrochlorination [13–15]. Also, nitrogen-doped in Cu-based catalysts for acetylene hydrochlorination can improve the acetylene adsorption and prolong the lifetime [16]. Combing the above results, it is demonstrated that dopants of nitrogen or phosphorus elements into Cu-based catalysts for acetylene hydrochlorination can strengthen the stability [13–18].

However, until now few studies researched the effect of nitrogen and phosphate elements on the catalytic performance of SnCl₂/AC catalysts for acetylene hydrochlorination. In this work, Sn(II)/PN@AC was prepared using the low-cost phosphoric acid, melamine, and SnCl₂ as phosphorus, nitrogen, and tin source, respectively.

* Correspondence: l63f64x@163.com

2. Materials and methods

2.1. Chemicals

Coal-based carbon carrier (AC, 40-60 meshes) was bought from Shanxi Xinhua Chemical Company. Melamine ($C_2H_4N_4$, $\geq 99.5\%$) and methyl orange was obtained from Tianjin Guangfu Technology Development Co., Ltd. Additionally, phosphoric acid (H_3PO_4 , $\geq 98.0\%$) was purchased from Sinopharm Chemical Reagent Co., Ltd. $SnCl_2 \cdot 2H_2O$ ($\geq 98.0\%$) was bought from Energy Chemical Co., Ltd. Moreover, Na_2CO_3 ($\geq 99.8\%$) was obtained from Tianjin Kernel Technology Development Co., Ltd. All materials were used without further purification.

2.2. Catalyst preparation

H_3PO_4 (0.54 g), $C_2H_4N_4$ (0.46 g), and AC (9.0 g) were firstly premixed in distilled water at 55 °C for 90 min, after which the sample was dried at 80 °C overnight. The obtained samples were calcinated at 550 °C for 4 h and then denoted as PN@AC. N@AC was prepared by the above-mentioned procedure.

Catalysts were prepared by the following processes. Firstly, $SnCl_2 \cdot 2H_2O$ (0.47 g) was completely dissolved in ethanol. Subsequently, $SnCl_2$ solution was gradually added to carbon supports, followed by air drying at 80 °C for 12 h. The above-mentioned described procedures were repeated to prepare 10%Sn(II)/PN@AC, 10%Sn(II)/N@AC, and 10%Sn(II)/AC, respectively.

2.3. Catalytic performance

The catalytic performance was tested in a fixed-bed quartz reactor (i.d.=10 mm). To remove water vapor, the reaction system was washed by hydrogen chloride for 30 min before the initial reaction. Then the gas mixture of HCl and C_2H_2 ($V_{C_2H_2}/V_{HCl} = 1.0:1.1$) was introduced into reactor containing 4.0 mL of catalysts with C_2H_2 -GHSV = 30 h^{-1} or 60 h^{-1} at 180 °C [19]. The final products contained the unreacted hydrogen chloride, which was adsorbed by the medical soda-lime. Having experienced adsorption, the cleaned gas mixture was analyzed online by GC900 (GDX-301 column).

2.4. Catalyst characterization

The BET surface area and pore textural properties data of the catalysts was acquired by a nitrogen adsorption method using Quantachrome Nova2000e instruments. The X-ray diffraction (XRD) patterns of the catalysts was collected from a Shimadzu XRD-6000 instrument using Cu K α radiation over the range of 10–80 °. Raman spectra of sample were performed on a Renishaw (514 nm laser source). Transmission electron microscopy (TEM) images were obtained using a JEM-2100F instrument with 300 keV acceleration voltages. X-ray photo-electron spectroscopy (XPS) analysis was conducted on an Esca Lab 250Xi spectrometer. Thermogravimetric analysis (TGA) experiments (NETZSCH STA 449F3 Jupiter instrument) carried out to study the coke deposition of catalysts. Inductively coupled plasma optical emission spectrometer (Agilent 720 ICP-OES) was used to determine the absolute content of tin elements in samples.

The Fourier transform infrared spectra (FT-IR) of the samples was measured by Biorad Excalibur FTS 3000). Acetylene temperature-programmed desorption (C_2H_2 -TPD) and hydrogen temperature-programmed reduction experiments (H_2 -TPR) were performed on FINESORB-3010 instruments, respectively [3]. Adsorption capacity of catalysts for HCl were calculated by the titration method [4].

3. Results and discussion

3.1. Characterization of supports

The structure of different supports was firstly studied, including the BET surface area and the pore volume. The value of AC (983.0 $m^2 \cdot g^{-1}$, 0.48 $m^3 \cdot g^{-1}$) was higher than that of N@AC (786.3 $m^2 \cdot g^{-1}$, 0.38 $m^3 \cdot g^{-1}$) and PN@AC (725.1 $m^2 \cdot g^{-1}$, 0.33 $m^3 \cdot g^{-1}$). It is demonstrated that the nonmetal additives are filled into the partial pores of AC (Figure 1a and Table 1). Figure 1b shows that the two diffraction peaks of AC were not affected by the introduction of nonmetal additives [20], inferring the well dispersion of promoter on AC surface [21]. As shown in Figure 1c, the I_D/I_G value gradually declines in the order of PN@AC(1.63) > N@AC(1.23) > AC (0.85), suggesting that PN-doping does lead to the more abundant defect of PN@AC and consequently improve the catalytic behavior of AC in acetylene hydrochlorination [22–24].

3.2. Characterization of Sn-based catalysts

As evident from Table 1 and Table 2, the load of $SnCl_2$ can reduce the specific surface area and the pore volume of supports. Furthermore, besides the characteristic peaks of carbon, the discernible peaks of $SnCl_2$ (PDF#72-0137) is not observed in tin-based catalysts (Figure 2a), inferring the dispersion of tin compounds on support surface [20,21]. As shown in Figures 2b and 2c, numerous black particles are dispersed on the support surface. Meanwhile, Figure 2d illustrates that no large particles are reunited on the PN@AC, indicating that Sn species are stably and homogeneously dispersed on the PN@AC.

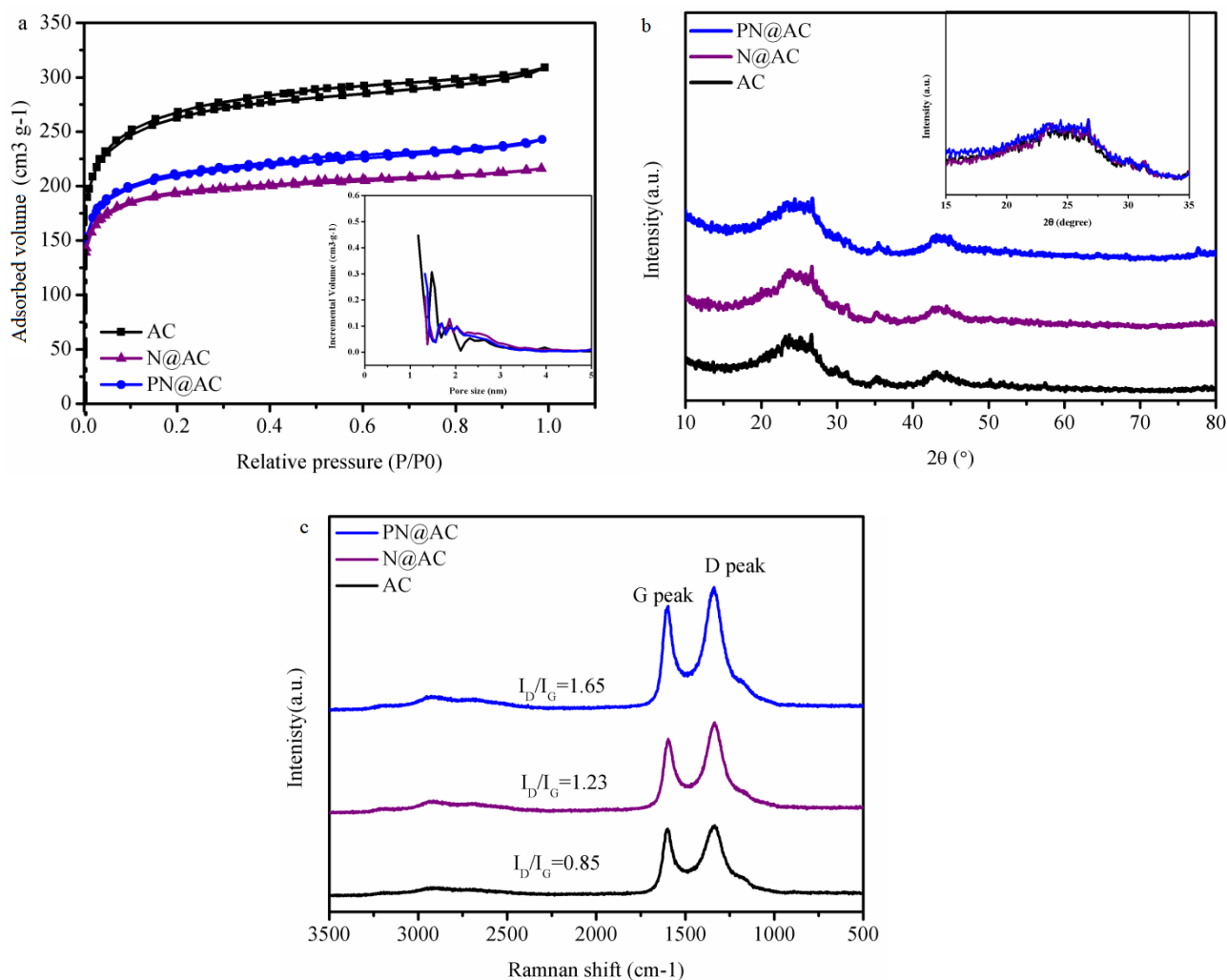


Figure 1. (a) N_2 adsorption-desorption isotherms of samples; (b) X-ray diffraction patterns of samples; (c) Raman spectra of samples.

Table 1. Textural properties of different catalysts.

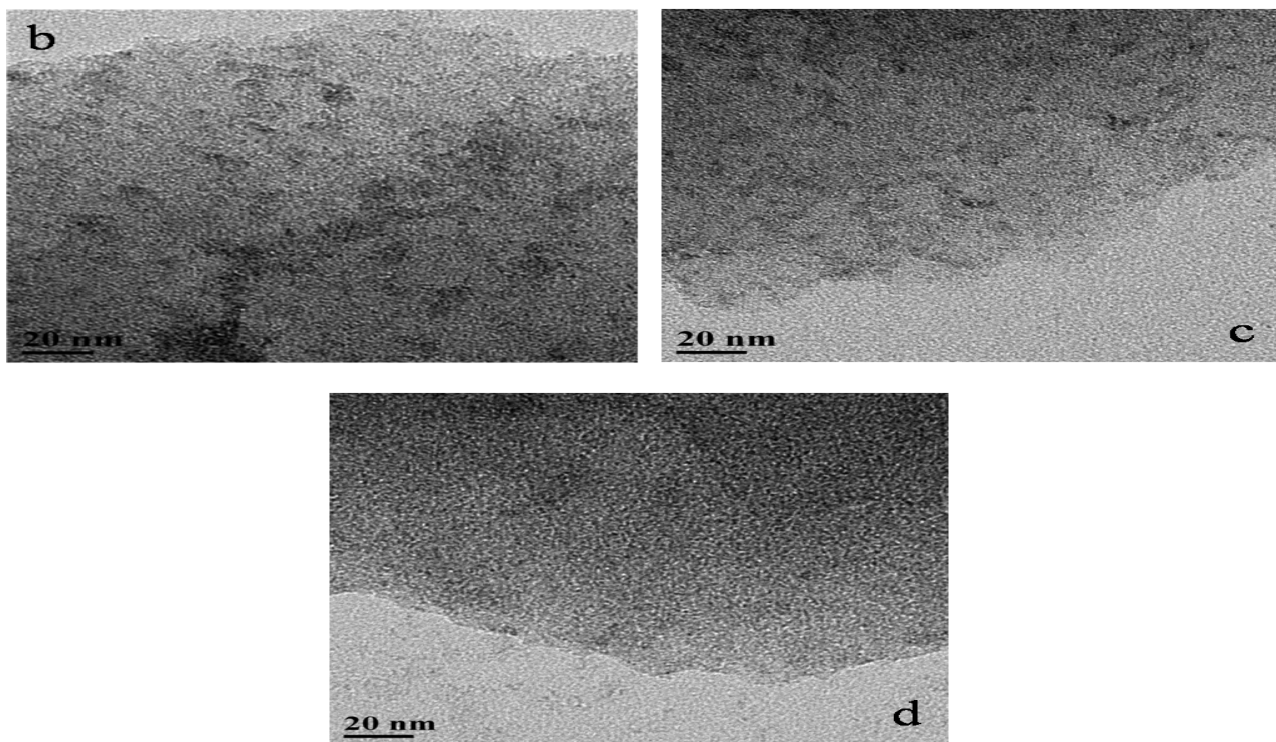
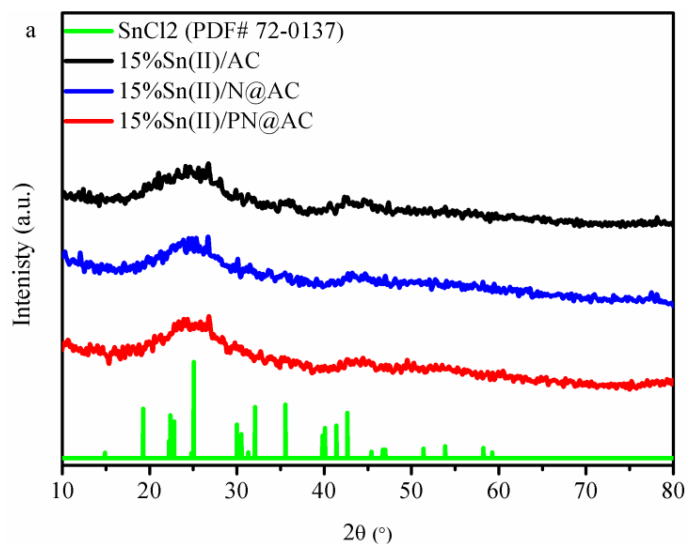
Samples	S_{BET} ($cm^2 g^{-1}$)	S_{micro} ($cm^2 g^{-1}$)	S_{meso} ($cm^2 g^{-1}$)	Total volume ($cm^3 g^{-1}$)	D (nm)
AC	983.0	853.9	129.1	0.48	1.9
N@AC	786.3	701.2	85.1	0.38	1.9
PN@AC	725.1	667.4	57.7	0.33	1.8
5%Sn(II)/PN@AC	547.8	485.6	62.2	0.26	1.9
10%Sn(II)/PN@AC	459.5	395.5	64.0	0.23	2.0
15%Sn(II)/PN@AC	303.3	203.2	67.9	0.20	2.1
20%Sn(II)/PN@AC	155.5	104.9	50.6	0.10	2.4

3.3. Catalytic performance

The catalytic performances of different catalysts were tested in acetylene hydrochlorination, and the results are shown in Figures 3a-c. The acetylene conversion on the Sn(II)/PN@AC increased as the $SnCl_2$ content (5 wt%–15 wt%). When the $SnCl_2$ content is 15 wt%, Sn(II)/PN@AC achieves an initial acetylene conversion of 100%, with vinyl chloride selectivity of

Table 2. Textural and structure properties of tin-based catalysts.

Sample	S_{BET} ($\text{m}^2\cdot\text{g}^{-1}$)		ΔS_{BET} ($\text{m}^2\cdot\text{g}^{-1}$)	V_{total} ($\text{m}^3\cdot\text{g}^{-1}$)	
	Fresh	Used		Fresh	Used
15%Sn(II)/AC	390.9	91.2	299.7	0.15	0.07
15%Sn(II)/N@AC	362.2	121.1	241.1	0.18	0.09
15%Sn(II)/PN@AC	303.3	164.7	138.6	0.20	0.14

**Figure 2.** (a) X-ray diffraction patterns of catalysts; TEM images of (b) 15%Sn(II)/AC, (c) 15%Sn(II)/N@AC, and (d) 15%Sn(II)/PN@AC.

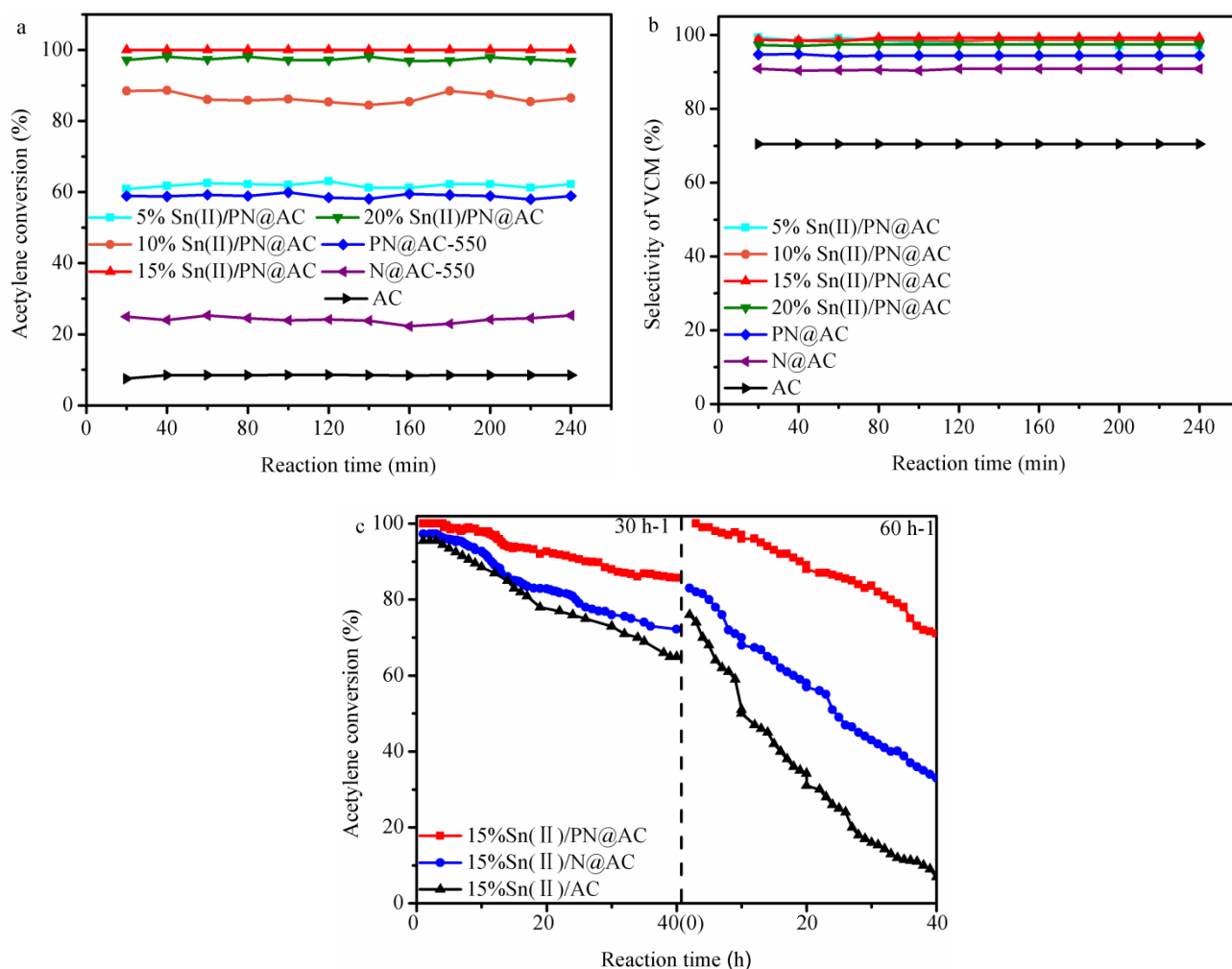


Figure 3. Acetylene conversion (a) and VCM selectivity (b) of catalysts (reaction conditions: $T = 180\text{ }^{\circ}\text{C}$, $\text{C}_2\text{H}_2\text{-GHSV}=30\text{ h}^{-1}$ and $V_{\text{HCl}}/V_{\text{C}_2\text{H}_2}=1.1/1.0$) (c) The stability of 15%Sn(II)/PN@AC, 15%Sn(II)/N@AC and 15%Sn(II)/AC (Reaction conditions: $T = 180\text{ }^{\circ}\text{C}$, $\text{C}_2\text{H}_2\text{-GHSV}=30\text{ h}^{-1}$ or 60 h^{-1} and $V_{\text{HCl}}/V_{\text{C}_2\text{H}_2}=1.1/1.0$)

98.5% (Figures 3a and 3b). It is noted that the acetylene conversion on 20%Sn(II)/PN@AC does not increase but decrease to 96.8%. However, Sn(II)/AC only behaved about 95.5% acetylene conversion (Figure 3c). At same time, the VCM selectivity of Sn(II)/PN@AC is over 98.0%. The results indicated that Sn(II)/PN@AC exhibited highly selectivity and catalytic activity in acetylene hydrochlorination. After 40 h reaction (Figure 3c), the acetylene conversion of 15%Sn(II)/AC is 62.1%, while the acetylene conversion of 15%Sn(II)/N@AC decreases from 97.3% to 72.2%, indicating that synergy between Sn species and N is one reason for the longer lifetime. Notably, 15%Sn(II)/PN@AC has an unusual catalytic stability in acetylene hydrochlorination reaction compared to 15%Sn(II)/AC catalysts with the same SnCl_2 loading, which indicates that the dual-elements (N and P) additives can further strengthen the stability of 15%Sn(II)/AC (Figure 3c). For 15%Sn(II)/N@AC and 15%Sn(II)/AC, the acetylene conversion under $\text{C}_2\text{H}_2\text{-GHSV}$ of 60 h^{-1} was 82.7% and 78.5%, respectively, while for 15%Sn(II)/PN@AC, the acetylene conversion under the same reaction condition (60 h^{-1}) was 99.7% (Figure 3c). Overall, 15%Sn(II)/PN@AC behaves the acetylene conversion of 99.0%, which meets the industrial production need ($\text{C}_2\text{H}_2\text{-GHSV}=30\text{ h}^{-1}\text{-}50\text{ h}^{-1}$ and $T = 130\text{ }^{\circ}\text{C}\text{-}180\text{ }^{\circ}\text{C}$) [25].

3.4. Synergistic effect between Sn and supports

The status of tin, nitrogen and phosphorus species in catalysts was characterized by XPS analysis (Figure 4a and Table 3). As Figure 4b illustrates, Sn-based catalysts behaved the two types of Sn species including Sn^{2+} ($\sim 486.7\text{ eV}$) and Sn^{4+} ($\sim 487.7\text{ eV}$) [26–28]. This result is consistent with $\text{H}_2\text{-TPR}$ results (Table 4). As shown in Figure 4e and Table 4, the H_2 reduction peaks of Sn^{2+} and Sn^{4+} in catalysts (15%Sn(II)/N@AC and 15%Sn(II)/PN@AC) was lower than the standard consumption

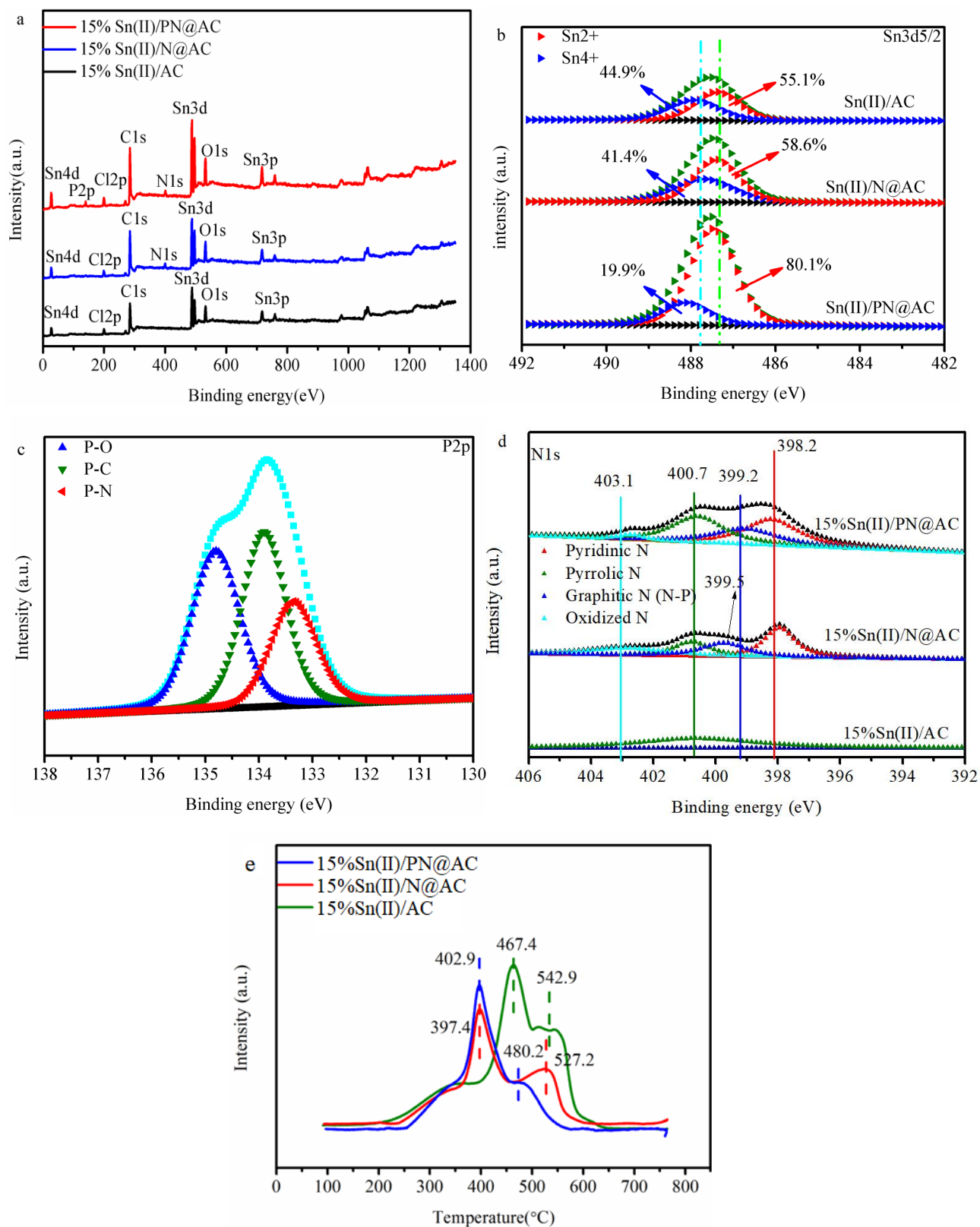


Figure 4. (a) XPS pattern of catalysts; (b) XPS-Sn_{3d_{5/2}} pattern of catalysts; (c) XPS-P_{2p} pattern of 15%Sn(II)/PN@AC; (d) XPS-N_{1s} pattern of catalysts; (e) H₂-TPR spectra of samples.

peaks (467.4 and 542.9 °C) [26–28], inferring that the nonmetal element additives can retard the oxidation of Sn²⁺ during the synthesis process and lessen the leach of Sn species during the reaction. The determination of Sn²⁺ and Sn⁴⁺ values in Tables (Table 4 and Table 5) was calculated on the normalization of peak areas. Figure 4c and Figure 4d confirm the existence of N-P and Pyridinic N, which can promote the reactivity of catalysts significantly [25,29,30]. The Pyridinic N content of 15%Sn(II)/N@AC was calculated to be 0.9 wt%, which is close to the 15%Sn(II)/PN@AC (0.88 wt%). It is revealed that phosphorus atoms bonded with nitrogen in the pyridine structure (ortho-position NP) is the main factor on the performance of 15%Sn(II)/AC according to the present work (Figure 1a, Figure 4d, and Table 6) and a recently published paper [25].

Table 3. Surface chemical element content of different catalysts by XPS.

Sample	Composition (wt%)					
	Sn	C	O	P	N	Cl
15%Sn(II)/AC	8.55	75.68	16.74	0.07	0.44	5.23
15%Sn(II)/N@AC	8.67	74.27	15.88	0.05	2.52	4.23
15%Sn(II)/PN@AC	8.90	72.66	16.42	0.91	2.43	4.64

Table 4. The relative peak area (TPR) of Sn²⁺ and Sn⁴⁺ in different tin-based catalysts.

Samples	Peak area (%)	
	Sn ²⁺	Sn ⁴⁺
15%Sn(II)/AC	53.2(467.4 °C)	45.8(542.9 °C)
15%Sn(II)/N@AC	69.7(397.4 °C)	30.3(527.2 °C)
15%Sn(II)/PN@AC	86.2(402.9 °C)	13.8 (480.2 °C)

Table 5. The content of Sn²⁺ and Sn⁴⁺ in different tin-based catalysts.

Sample	Composition (wt %)		
	Total Sn	Sn ⁴⁺	Sn ²⁺
15%Sn(II)/AC	4.55	2.04	2.51
15%Sn(II)/N@AC	4.67	1.93	2.74
15%Sn(II)/PN@AC	4.90	0.98	3.92

Table 6. Chemical composition of the N1s in different tin-based catalysts (XPS).

Samples	Composition (wt %)				
	Total N	Pyridinic N	Graphitic N	Pyrrolic N	Oxidized N
15%Sn(II)/AC	0.44	--	0.44	--	--
15%Sn(II)/N@AC	2.52	0.90	0.81	0.64	0.17
15%Sn(II)/PN@AC	2.43	0.88	0.84	0.62	0.09

As shown in Figure 4c, the electron binding energies at 135.0 eV, 133.5 eV, and 132.6 eV can be assigned to P-O, P-N, and P-C [23,24,31]. Particularly, the addition of SnCl_2 into catalysts shift the P-N binding energy from 133.5 eV to 133.2 eV. Moreover, a positive shift (0.3 eV) can be observed in the binding energy of Sn^{2+} for 15%Sn(II)/PN@AC versus 15%Sn(II)/AC. Therefore, it is attributing this shift to the synergistic effect between ortho-position NP and Sn species [32,33].

3.5 Synergistic effect between Sn and reactants

To study the effect of various adsorption reactants on the structural conformation of SnCl_2 , we used FT-IR techniques to analyze three samples including Sn(II)/AC- C_2H_2 , Sn(II)/AC-HCl, and Sn(II)/AC- N_2 (Figure 5), which represent that SnCl_2 /AC was respectively pretreated at 200 °C for 1 h under acetylene, hydrogen chloride, and nitrogen atmosphere, respectively. Two characteristic adsorption bands at $\sim 1121\text{ cm}^{-1}$ and $\sim 3397\text{ cm}^{-1}$ are observed in Sn(II)/AC-HCl, suggesting that the gaseous HCl reacted firstly with Sn species. Figure 4a shows that Sn(II)/AC catalysts during acetylene hydrochlorination contains SnCl_4 and SnCl_2 , the latter of which is the main formation of Sn species. Based on the analysis of our previous study [3], owing to SnCl_4 and HCl are electron-receptor, the adsorption of HCl on the SnCl_2 sites forms the HSnCl_3 [34–36]. The results of FT-IR spectra are no obvious difference between Sn(II)/AC- N_2 and Sn(II)/AC- C_2H_2 , implying that SnCl_2 cannot make bond with C_2H_2 . Combining the Eley–Rideal mechanism and previous work [34–38], it is indicated that HSnCl_3 is as transition state of SnCl_2 in the catalysis of acetylene hydrochlorination.

HCl adsorption experiments was applied to study the HCl adsorption capacity of catalysts, and the results are displayed in Figure 6a. The adsorption capacity of HCl on 15%Sn(II)/PN@AC, 15%Sn(II)/N@AC, and 15%Sn(II)/AC are 0.64

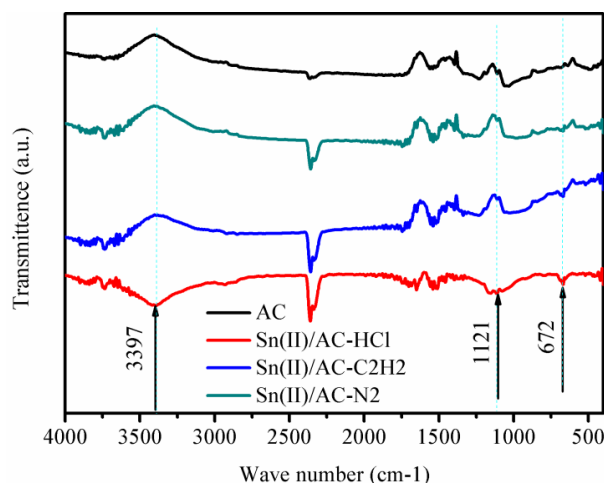


Figure 5. FT-IR spectra of samples.

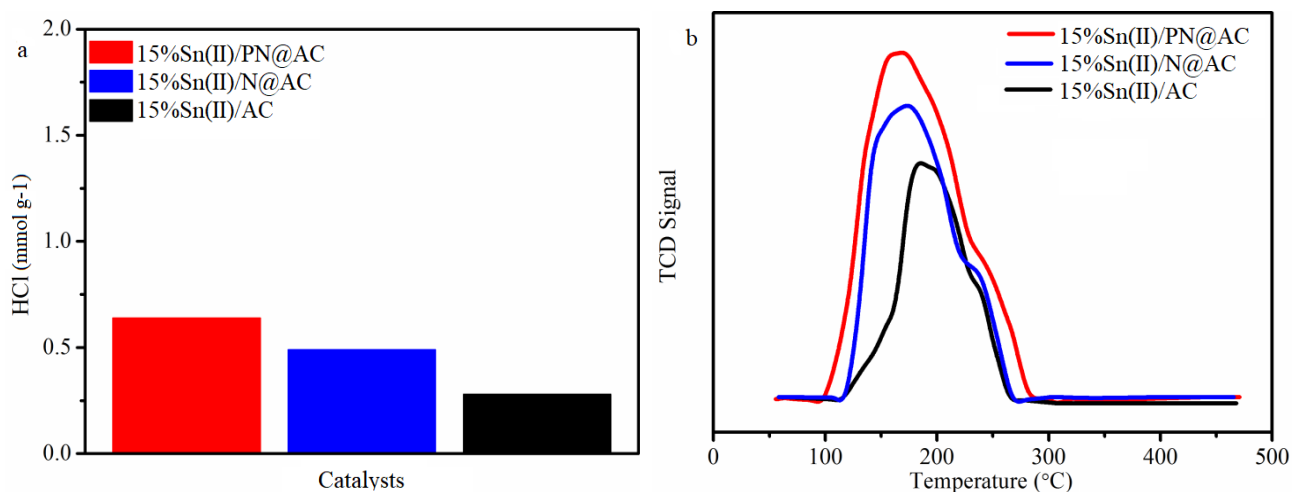


Figure 6. (a) HCl adsorption and (b) C_2H_2 -TPD profile of catalysts.

mmol·g⁻¹, 0.49 mmol·g⁻¹, and 0.28 mmol·g⁻¹, respectively. The published papers find that HCl adsorbs on Pyridinic N firstly [30], but the Pyridinic N content in 15%Sn(II)/PN@AC is close to 15%Sn(II)/N@AC (Table 6). It is implying that the synergy effect between Sn and NP may be responsible for the highly HCl adsorption capacity and thus improve the catalytic behaviors of tin-based catalysts in acetylene hydrochlorination, based on the above results.

As shown in Figure 6b, the adsorption area for C₂H₂ of catalysts decreases in the order 15%Sn(II)/PN@AC > 15%Sn(II)/N@AC > 15%Sn(II)/AC. When N and P-codoped 15%Sn(II)/AC can result in higher C₂H₂ adsorption capacity as compare to 15%Sn(II)/N@AC and 15%Sn(II)/AC. This result indicates that NP is responsible for the C₂H₂ adsorption capacity, which is well agree with the previous study [25].

3.6 Inactivation of tin-based catalysts

After 40 h reaction, the reduction of BET surface area in used tin-based catalysts is listed in Table 2, the loss of BET surface area in 15%Sn(II)/PN@AC, 15%Sn(II)/N@AC and 15%Sn(II)/AC reaches 138.6 m²·g⁻¹, 241.1 m²·g⁻¹, and 299.7 m²·g⁻¹. Figure 7 shows the TGA curves of catalysts before and after reaction. Based on the same type fresh- and used-catalysts, the weight loss in the temperature range of 150–470 °C was mainly originated from the coke deposition on the catalysts surface in acetylene hydrochlorination [39,40], and the results is listed in Table 7. The amount of coke deposition for the 15%Sn(II)/PN@AC, 15%Sn(II)/N@AC, and 15%Sn(II)/AC catalysts are 1.70%, 3.61%, and 3.70% (Figures 7a and b). Thus, the synergistic effect of Sn species and NP in 15%Sn(II)/PN@AC can accelerate the anti-coking ability, which, consequently, prolonging the lifetime of the Sn-based catalysts. The 75.9%, 72.3%, and 65.4% of the initial Sn content is lost from 15%Sn(II)/AC, 15%Sn(II)/N@AC, and 15%Sn(II)/PN@AC, respectively, after 40 h reaction (Table 8), demonstrating that the leach of tin species is a deactivation reason of tin-based catalysts and manifesting that NP additives can retard the loss of tin compounds during acetylene hydrochlorination[41].

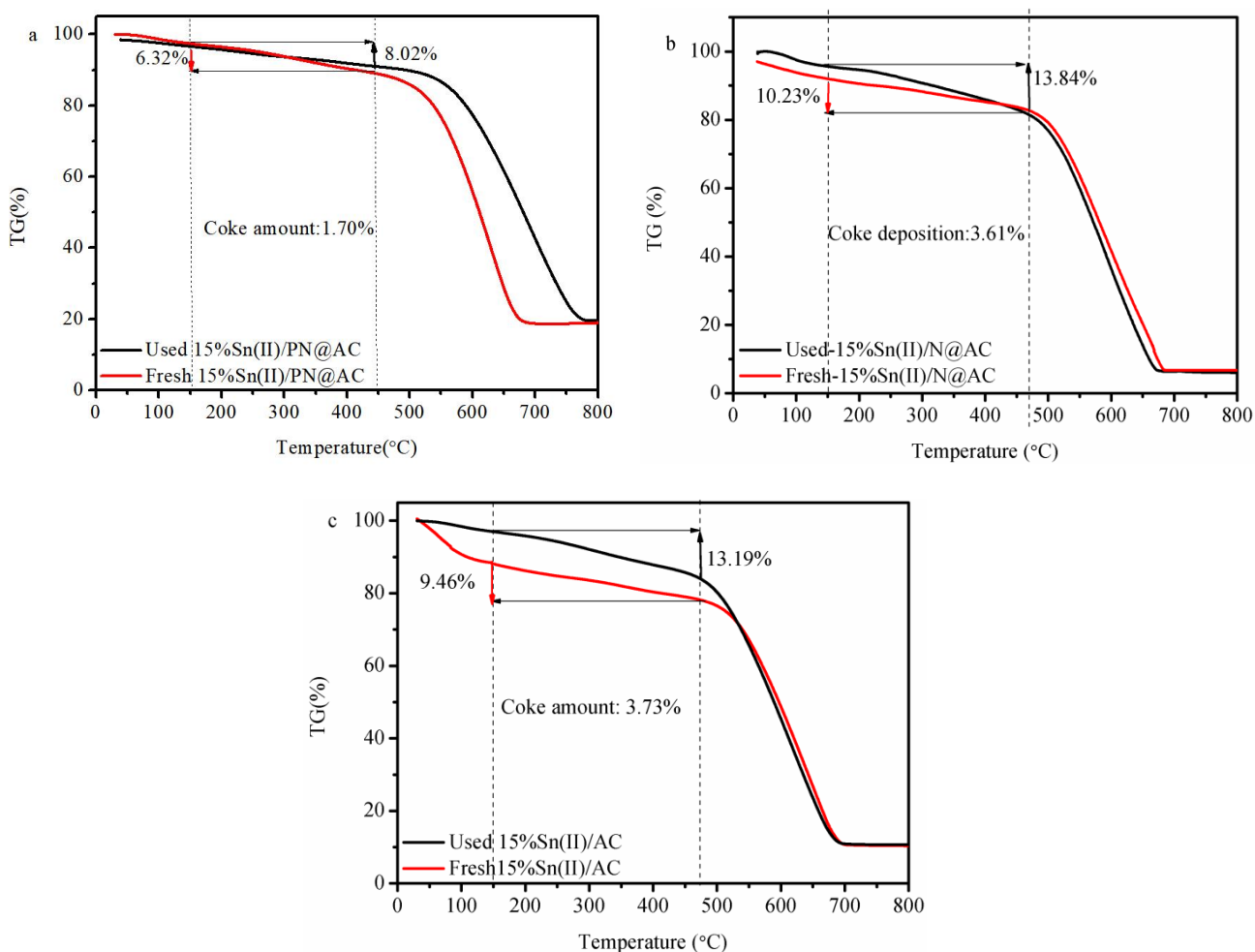


Figure 7. TG curves of catalysts: (a) 15%Sn(II)/PN@AC; (b) 15%Sn(II)/N@AC; (c) 15%Sn(II)/AC.

Table 7. Coke deposition of catalysts.

Samples	Coke deposition (%)
15%Sn(II)/AC	3.73
15%Sn(II)/N@AC	3.61
15%Sn(II)/PN@AC	1.70

Table 8. The content of Sn in fresh and used tin based catalysts determined by different method.

Samples	Nominal ^a (wt%)	ICP (wt%)		Loss ratio of Sn (%)
		Fresh	Used	
15%Sn(II)/AC	8.5	8.3	2.0	75.9%
15%Sn(II)/N@AC	8.5	8.3	2.3	72.3%
15% Sn(II)/PN@AC	8.5	8.1	2.8	65.4%

^aTheoretical calculation method: $M(\%) = (M_{\text{sn species}}/M_{\text{sn}})/(M_{\text{catalysts}})$.
 $M_{\text{sn species}}$: the weight of Sn species; M_{sn} : 225 g/mol; $M_{\text{catalysts}}$: the weight of catalysts.

4. Conclusion

Although carbon supported-HgCl₂ as catalyst exhibits considerable catalytic performance, its toxicity and sublimation can be led to the serious environmental pollution. Additionally, the Minamata convention will be forbidden the utilization of mercury-based materials. But this study reported that Sn/PNAC as catalysts for acetylene hydrochlorination was prepared using nontoxic compounds. This work also finds that the stability of 15%Sn(II)/PN@AC catalysts correlate with N and P additives. After careful characterizations and additional catalytic tests, PN@AC supports can not only make the tin compounds dispersion well, but also strengthens the reactants adsorption of catalysts. According to the XPS, C₂H₂-TPD, H₂-TPR, and HCl adsorption experiments results, it is found that the better catalytic behavior of Sn(II)/PN@AC is mainly attributed to the synergy between ortho-position NP and Sn species. Additionally, the reaction mechanism was proposed as follows, the adsorption of HCl on SnCl₂ forms the transition state (HSnCl₃) is the initial step and then react with C₂H₂ to produce the vinyl chloride. Such a finding provides the guidance to develop the tin-based catalysts for acetylene hydrochlorination.

Acknowledgment

This work is supported by PhD research startup foundation of Pingding Shan University (PXY-BSQD-202110)

References

- Li Q, Fu JJ, Zhu WL, Chen ZZ, Shen B et al. Tuning Sn-catalysis for electrochemical reduction of CO₂ to CO via the core/shell Cu/SnO₂ structure. *Journal of the American Chemical Society* 2017; 139: 4290-4293. doi: 10.1021/jacs.6b00261
- Deng GC, Wu BX, Li TS, Liu GD, Wang LF et al. Preparation of solid phase non-mercury catalyst for the synthesis of vinyl chloride by acetylene. *Polyvinyl Chloride* 1994; 6: 5-9.
- Wu YB, Li FX, Lv ZP, Xue JW. Carbon-supported binary Li-Sn catalyst for acetylene hydrochlorination. *Journal of Saudi Chemical Society* 2019; 23: 1219-1230. doi: 10.1016/j.jscs.2019.08.002
- Wu YB, Li FX, Xue JW, Lv ZP. Sn-imidazolates supported on boron and nitrogen-doped activated carbon as novel catalysts for acetylene hydrochlorination. *Chemical Engineering Communications* 2019; 207: 1203-1215. doi: 10.1080/00986445.2019.1641700
- Guo YY, Liu Y, Hu RS, Gao GJ, Sun HJ. Preparation and optimization of SnCl₂-ZnCl₂/C mercury-free catalyst for acetylene hydrochlorination. *Chinese Journal of Applied Chemistry* 2014; 31: 624-626. doi: 10.3724/SP.J.1095.2014.30337
- Zhang L, Jiang H, Wang H, Dong SW, Ding QW et al. Preparation and application of non-mercury catalysts for acetylene hydrochlorination. *Journal of Petrochemical Universities* 2013; 26: 6-11. doi: 10.3969/j.issn.1006-396X.2013.06.002

7. Xiong Q, Wu GW, Leng S, Xiong Z, Hu ZP et al. Preparation and optimization of mercury-free catalysts for the synthesis of vinyl chloride from acetylene. *Modern Chemistry* 2017; 37: 66-69. doi:10.16606/j.cnki.issn0253-4320.2017.11.015
8. Gao SL, Sun X, Lv ZL, Qin YC, Zhang XT et al. The application of Sn-Bi-Co@AC catalysts for acetylene hydrochlorination. *Journal of Petrochemical Universities* 2016; 2: 1-5. doi: 10.3969/j.issn.1006-396X.2016.02.001
9. Wu YB, Li BW, Li FX, Xue JW, Lv ZP. Synthesis and characteristics of organotin-based catalysts for acetylene. *Canadian Journal of Chemistry* 2018; 96: 447-452. doi: 10.1139/cjc-2017-0612
10. Wu YB, Cui LJ, Zhang R, Pei RJ, Hu SF et al. $\text{Ph}_n\text{SnCl}_{4-n}$ supported on activated carbon as novel tin-based catalysts for acetylene hydrochlorination. *Química Nova* 2019; 42: 752-759. doi: 10.21577/0100-4042.20170390
11. Wu YB, Li FX, Xue JW, Lv ZP. Effect of various g- C_3N_4 precursors on the catalytic performance of alkylorganotin-based catalysts in acetylene hydrochlorination. *Turkish Journal of Chemistry* 2020; 44: 393-408. doi: 10.3906/kim-1909-64
12. Wu YB, Li FX, Lv ZP, Xue JW. Synthesis and characterization of X-MOF/AC (X=tin or copper) catalysts for the acetylene hydrochlorination. *Chemistry Select* 2019; 4: 9403-9409. doi: 10.1002/slct.201902017
13. Wang XM, Zhu MY, Dai B. Effect of phosphorus ligand on Cu-based catalysts for acetylene hydrochlorination. *ACS Sustainable Chemistry & Engineering* 2019; 7: 6170-6177. doi: 10.1021/acssuschemeng.8b06379
14. Ren YF, Wu BT, Wang FM, Li H, Lv GJ et al. Chlorocuprate (i) ionic liquid as an efficient and stable Cu-based catalyst for hydrochlorination of acetylene. *Catalysis: Science and Technology* 2019; 9: 2868-2878. doi: 10.1039/c9cy00401g
15. Hu YB, Wang Y, Wang YL, Li W, Zhang JL et al. High performance of supported Cu-based catalysts modulated via phosphamide coordination in acetylene hydrochlorination. *Applied Catalysis, A: General* 2020; 591: 117408. doi: 10.1016/j.apcata.2020.117408
16. Zhao WL, Zhu MY, Dai D. The Preparation of Cu-g- C_3N_4 /AC catalyst for acetylene hydrochlorination. *Catalysts* 2016; 6: 193. doi: 10.3390/catal6120193
17. Wang Y, Nian Y, Zhang JL, Li W, Han Y. MOMTPPC improved Cu-based heterogeneous catalyst with high efficiency for acetylene hydrochlorination. *Molecular Catalysis* 2019; 479: 110612. doi: 10.1016/j.mcat.2019.110612
18. Zhou K, Si JK, Jia JC, Huang JQ, Zhou J et al. Reactivity enhancement of N-CNTs in green catalysis of C_2H_2 hydrochlorination by a Cu catalyst. *RSC Advances* 2014; 4: 7766. doi: 10.1039/C3RA46099A
19. Zhao J, Wang B, Yue Y, GF Sheng, HX Lai et al. Nitrogen- and phosphorus-codoped carbon-based catalyst for acetylene hydrochlorination. *Journal of Catalysis* 2019; 373: 240-249. doi: 10.1016/j.jcat.2019.03.044
20. Qian HS, Han FM, Zhang B, Guo YC, Yun J et al. Non-catalytic CVD preparation of carbon spheres with a specific size. *Carbon* 2004; 42: 761-766. doi: 10.1016/j.carbon.2004.01.004
21. Dong YZ, Zhang HY, Li W, Sun MX, Guo CL et al. Bimetallic Au-Sn/AC catalysts for acetylene hydrochlorination. *Journal of Industrial and Engineering Chemistry* 2016; 35: 177-184. doi: 10.1016/j.jiec.2015.12.031
22. Choi CH, Chung MW, Kwon HC, Park SH, Woo SI. B, N- and P, N-doped graphene as highly active catalysts for oxygen reduction reactions in acidic media. *Journal of Materials Chemistry* 2013; 1: 3694-3699. doi: 10.1039/c3ta01648j
23. Zhang JT, Qu LT, Shi GQ, Liu JY, Chen JF et al. N,P-codoped carbon networks as efficient metal-free bifunctional catalysts for oxygen reduction and hydrogen evolution reactions. *Angewandte Chemie, International Edition* 2016; 55: 2230-2234. doi: 10.1002/anie.201510495
24. Zhao J, Wang BL, Yue YX, Sheng GF, Lai HX et al. Nitrogen- and phosphorous-co doped carbon-based catalyst for acetylene hydrochlorination. *Journal of Catalysis* 2019; 373: 240-249. doi: 10.1016/j.jcat.2019.03.044
25. Li XY, Pan XL, Yu L, Ren PJ, Wu X et al. Silicon carbide-derived carbon nanocomposite as a substitute for mercury in the catalytic hydrochlorination of acetylene. *Nature Communications* 2014; 5: 3688. doi: 10.1038/ncomms4688
26. Pham HN, Sattler JJHB, Weckhuysen BM, Datye AK. Role of Sn in the regeneration of Pt/ $\gamma\text{-Al}_2\text{O}_3$ light alkane dehydrogenation catalysts. *ACS Catalysis* 2016; 6: 2257-2264. doi: 10.1021/acscatal.5b02917
27. Zhang YW, Zhou YM, Wan LH, Xue MW. Influence of the different dechlorination time on catalytic performances of PtSnNa/ZSM-5 catalyst for propane dehydrogenation. *Fuel Processing Technology* 2011; 90: 1524-1531. doi: 10.1016/j.fuproc.2009.07.019
28. Afonso JC, Aranda DAG, Schmal M, Frety R. Importance of pretreatment on regeneration of a Pt-Sn/ Al_2O_3 catalyst. *Fuel Processing Technology* 1995; 42: 3-17. doi: 10.1016/0378-3820(94)00103-Z
29. Lin R, Kaiser SK, Hauert R, Pérez-Ramírez J. Descriptors for high-performance nitrogen-doped carbon catalysts in acetylene hydrochlorination. *ACS Catalysis* 2018; 8: 1114-1121. doi: 10.1021/acscatal.7b03031
30. Li XN, Wang Y, Kang LH, Zhu MY, Dai B. A novel, non-metallic graphitic carbon nitride catalyst for acetylene hydrochlorination, *Journal of Catalysis* 2014; 311: 288-294. doi: 10.1016/j.jcat.2013.12.006

31. Kobayashi Y, Salgueirino V, Liz-Marzán LM. Deposition of silver nanoparticles on silica spheres by pretreatment steps in electroless plating. *Chemistry of Materials* 2001; 13: 1630-1633. doi: 10.1021/cm001240g
32. Liu ZL, Wang XX, Wu ZY, Yang SJ, Yang SL et al. Ultrafine Sn₄P₃ nanocrystals from chloride reduction on mechanically activated Na surface for sodium/lithium ion batteries. *Nano Research* 2020; 13: 3157-3164. doi: 10.1007/s12274-020-2987-2
33. Lewin E, Patscheider J. Structure and properties of sputter-deposited Al-Sn-N thin films. *Journal of Alloys and Compounds* 2016; 682: 42-51. doi: 10.1016/j.jallcom.2016.04.278
34. Du JH, Feng LP, Guo X, Huang XP, Lin ZH et al. Enhanced efficiency and stability of planar perovskite solar cells by introducing amino acid to SnO₂/perovskite interface. *Journal of Power Sources* 2020; 455: 22974. doi: 10.1039/C7TA04014H
35. Kowalewska E, Błażejowski J. Thermochemical properties of H₂SnCl₆ complexes. part I. thermal behaviour of primary n-alkylammonium hexachlorostannates. *Thermochimica Acta* 1986; 101: 271-289. doi: 10.1016/0040-6031(86)80059-4
36. Thangaraju B. Structural and electrical studies on highly conducting spray deposited fluorine and antimony doped SnO₂ thin films from SnCl₂ precursor. *Thin solid films* 2002; 402: 71-78. doi: 10.1016/S0040-6090(01)01667-4
37. Bremer H, Lieske H. Kinetics of the hydrochlorination of acetylene on HgCl₂/active carbon catalysts. *Applied Catalysis A-General* 1985; 18: 191-203. doi: 10.1016/S0166-9834(00)80308-5
38. Wang HJ, Sun FQ, Zhang Y, Li LS, Chen HY et al. Photochemical growth of nanoporous SnO₂ at the air-water interface and its high photocatalytic activity. *Journal of Materials Chemistry* 2010; 20: 5641-5645. doi: 10.1039/B926930D
39. Zhang HY, Dai B, Wang XG, Li W, Han Y et al. Non-mercury catalytic acetylene hydrochlorination over bimetallic Au-Co(III)/SAC catalysts for vinyl chloride monomer production. *Green Chem* 2013; 15: 829-836. doi: 10.1039/C4CY01399A
40. Zhang HY, Dai B, Wang XG, Xu LL, Zhu MY. Hydrochlorination of acetylene to vinyl chloride monomer over bimetallic Au-La/SAC catalysts. *Journal of Industrial and Engineering Chemistry* 2012; 18: 49-54. doi: 10.1016/j.jiec.2011.11.075
41. Dai B, Chen K, Wang Y, Kang LH, Zhu MY. Boron and nitrogen doping in graphene for the catalysis of acetylene hydrochlorination. *ACS Catalysis* 2015; 5: 2541-2547. doi: 10.1021/acscatal.5b00199